05.2;06.5

Features of formation of structure and properties of Mn−Zn ferrites obtained by sol-gel synthesis method

© R.R. Khabirov, A.V. Mass, R.I. Kuzmin, A.A. Ruktuev, N.Yu. Cherkasova, M.Yu. Agafonov, V.A. Koroleva, A.A. Miller

Novosibirsk State Technical University, Novosibirsk, Russia
E-mail: xabirov.2016@stud.nstu.ru

Received December 11, 2023
Revised January 9, 2024
Accepted January 26, 2024

The influence of sol-gel synthesis as an initial stage of Mn−Zn ferrites production on their structure and properties is shown. The used method allowed to obtain sintered material with uniform grain structure, to increase density, initial magnetic permeability and maximum induction, to reduce magnetic losses.

Keywords: Mn−Zn ferrite, sol-gel, microstructure, magnetic permeability, magnetic losses.

DOI: 10.61011/TPL.2024.05.58414.19834

Ceramic technology is used in the mass production of Mn−Zn ferrites for electronics. The weak side of this technology is the insufficiently uniform distribution of components in case of mixing of oxide powders [1]. A considerable attention has been paid recently to chemical synthesis methods, since mixing solutions of metal salts at the molecular level allows obtaining a homogeneous distribution of components[2]. The uniformity of the distribution has a significant impact on the formation of the microstructure of [3], therefore, the chemical synthesis of powders can become a promising method for obtaining ferrites with a high level of magnetic properties. The sol-gel technology is a promising method for the synthesis of ceramic powders [4]. This method allows a precise control of the chemical composition and structural characteristics of synthesized materials [5]. Thew powders with a high concentration of ferrite are formed as a result of sol-gel synthesis according to studies [6,7]. The phase composition has a significant effect on the pre-heat treatment, grinding and sintering. For instance, the authors of Ref. [8] found that sintering powders with a high ferrite content increases the magnetic permeability and reduces the magnetic losses of Mn−Zn ferrites.

The chemical synthesis methods are often used in the modern literature to produce nanopowders of Mn−Zn ferrites. At the same time, ferrites produced by sintering from such powders have not been sufficiently studied. It was shown in [9] that the average grain size and saturation magnetization of ferrite increase with an increase of the sintering temperature of powders obtained using sol-gel synthesis. The microstructure, saturation magnetization, and coercive force of Mn-, Ni-, and Cu-ferrites with different Zn contents were studied in [10]. However, little attention was paid to the comparative analysis of the features of the formation of the grain structure of ferrites obtained using chemical synthesis and ceramic technology. There is also insufficient data on the effect of the powder synthesis method on the magnetic permeability and magnetic losses of bulk materials from Mn−Zn ferrites. The impact of sol-gel synthesis as the initial stage of the manufacture of Mn−Zn ferrites on the microstructure and properties of sintered materials was evaluated in this paper.

Samples of ferrites of the composition $Mn_{0.65}Zn_{0.28}Fe_{2.08}O_4$ were obtained without additives and with an addition of 0.035 mass% of Co_3O_4 and 0.05 mass% of CaO. Powders of Fe_2O_3, $MnCo_3$, ZnO, Co_3O_4, CaO (purity 99.5%) were used for the oxide technology. Mixing was performed in a ball mill in an aqueous medium. The dried mixture was calcined at 1000° C with exposure for 2 h in air, wet grinding was performed in a ball mill, granulated by drying with the addition of 1 mass% polyvinyl alcohol. Annular samples with size of $20 \times 10 \times 5$ mm were obtained from the resulting granular powder by axial pressing. The blanks were calcined at 700°C to remove organic additives. Sintering was performed at 1300°C with heating and exposure (3 h) in air and cooling in vacuum.

Powders of $FeSO_4 \cdot 7H_2O$, $MnSO_4 \cdot 5H_2O$, $ZnSO_4 \cdot 7H_2O$, $CoSO_4 \cdot 7H_2O$, $Ca(NO_3)_2 \cdot 4H_2O$ (chemically pure) were used as raw materials for chemical synthesis. A solution of metal salts was mixed with citric acid and ammonia until reaching pH = 7. The sol was dried at 100°C, heated to self-ignition producing a fine powder. The powders were calcined at 1000°C in air, milled, granulated, pressed and sintered in accordance with the conditions described above. The microstructure of ferrites was studied using a Carl Zeiss Axio Observer Z1m optical microscope, X-ray phase analysis was performed using Adwin POWDIX 600 diffractometer with CuK_α-radiation, density ρ was measured by hydrostatic weighing method. The initial magnetic permeability of μ_i is determined by measuring the inductance of annular cores with a copper cable winding. $B-H$-analyzer DX-2012SA (DEXINMAG) was used to measure the maximum magnetic induction B_m in a field with a strength of $H_m = 1200$ A/m and magnetic losses. A full-profile analysis of diffraction patterns using the Rietveld

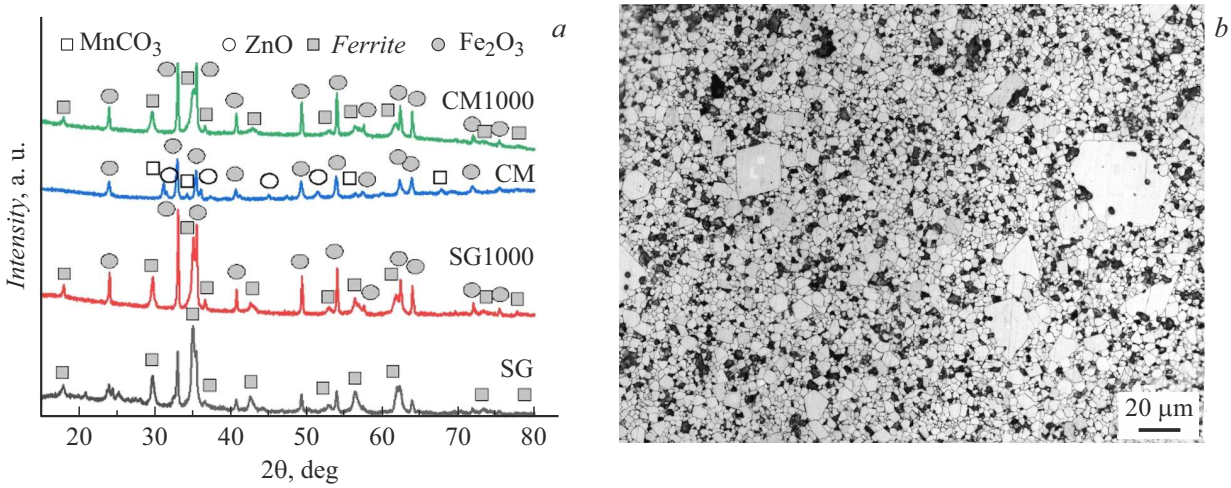

Figure 1. *a* — diffraction patterns of ferrite powders after calcination at 1000°C, obtained using sol-gel (SG1000) and ceramic (CM1000) method, as well as sol-gel powder (SG) and oxide mixture (CM) before calcination; *b* — the microstructure of sintered ferrite obtained using ceramic technology.

method using the software Maud 2.9993 was carried out to determine the phase composition, the size of the crystallite size, the parameters of the crystal lattice, the volume of the unit cell and the theoretical density of the phases [11]. The ICDD PDF 4+ database was used to decipher the phase composition.

The powder after sol-gel synthesis has a crystalline structure and contains a ferrite phase (Fig. 1, *a*). On the contrary, the powder mixture obtained by the oxide mixing consists only of the phases of the initial components: α-Fe_2O_3 (ICDD 04-002-7501), ZnO (ICDD 04-008-8199), $MnCO_3$ (ICDD 04-001-7250). The powder consists of ferrite (ICDD 01-074-2400) and α-Fe_2O_3 (ICDD 01-089-0597) after calcination at 1000°C in both cases. Iron oxide is present because of - incomplete completion of the ferrite formation reaction at 1000°C, as well as a result of the decay of $MnFe_2O_4$, unstable in air at temperatures below 1000°C [12]. However, the powder obtained by calcination of a mixture of oxides is larger (50 mass.% of particles remain on a sieve with a mesh size of 250 μm) compared to the powder synthesized from salts (10 mass% of particles remain on a sieve with a cell of 250 μm). Probably, the process of aggregation and growth of particles during heat treatment is more active in a mixture of oxides because of the close location of the particles obtained by evaporation of water from the suspension. This is confirmed by the fact that the size of the crystallite size of ferrite and α-Fe_2O_3 phases in powders obtained by mixing oxides is higher than the size of the crystallite size after sol-gel synthesis (Table 1). Sol-gel synthesis affects not only on the size of the powder particles, but also on the course of phase transformations and the chemical composition of the phases. This is confirmed by the higher concentration of the ferrite phase and the parameters of the crystal lattice and the lower theoretical density of powders obtained using sol-gel synthesis (Table 2). The grinding was performed under the same conditions in a ball mill for 10 h. The amount of ferrite in all powders decreases by an average of 2,mass% after grinding. As reported in [13], this may occur as a result of the decay of the metastable $MnFe_2O_4$, which is caused by mechanical stresses. The size of the crystallite size of ferrite and α-Fe_2O_3 after grinding for all powders decreases because of - an increase in the number of defects in the powder particles. A decrease of crystallite size during grinding was recorded in [14]. It is known [15], that the specific surface area increases as the particle size decreases, which accelerates the sintering processes. The parameters of the crystal lattice and the volume of the lattice cell of the ferrite and α-Fe_2O_3 phases of powders obtained by the ceramic method increase and the theoretical density decreases after grinding. The inverse dependence is observed in materials synthesized using the sol-gel method (Table 2). The authors of Ref. [16] concluded that the grinding process involves processes that affect the parameters of the crystal lattice in different ways. On the one hand, the mechanical impact of the grinding media should result an increase of compressive stresses in the powder particles and a decrease of the lattice parameters. On the other hand, the accumulation of defects in the crystal lattice and the redistribution of cations along the sublattices of spinel can increase its parameters.

The density of ferrites obtained by the sol-gel method is 2.5–5% higher than that of those made from oxides (Table 3). The maximum induction B_m increases with the increase of density in ferrites of the same composition. The ferrite obtained by the ceramic method has a fine-grained structure, while the presence of 2.5 vol.% of abnormally large grains (average size 80,μm) indicates secondary recrystallization (Fig. 1, *b*). The volume fraction of abnormally large grains increased to 8.8 vol.%, the average size increased to 100 μm, the average grain size, excluding abnormally large ones, decreased (Fig. 2, *a*) when 0.035 mass% Co_3O_4 and 0.05 mass% CaO were introduced into ferrite obtained from oxides. On the one

Table 1. Crystallite size and phase composition of ferrite powders calcined at 1000°C

Method	crystallite size, nm		Phase composition	
	Fe_2O_3	Ferrite	Fe_2O_3	Ferrite
Ceramic Method	154 ± 5	102 ± 1	50 ± 1	50 ± 1
Ceramic method, grinding 10 h	120 ± 2	91 ± 3	52 ± 1	48 ± 1
Ceramic method + Co_3O_4 + CaO	119 ± 2	63 ± 4	52 ± 1	48 ± 1
Ceramic method + Co_3O_4 + CaO, grinding 10 h	94 ± 2	73 ± 8	54 ± 1	46 ± 1
Sol-gel	110 ± 2	87 ± 10	48 ± 1	52 ± 1
Sol-gel, grinding 10 h	98 ± 1	45 ± 3	52 ± 1	48 ± 1
Sol-gel + Co_3O_4	108 ± 2	44 ± 1	48 ± 1	52 ± 1
Sol-gel + Co_3O_4 + CaO, grinding 10 h	80 ± 1	32 ± 1	52 ± 1	48 ± 1

Table 2. Lattice parameters, unit cell volume and theoretical density of ferrite powders calcined at 1000°C

Method	Lattice parameters, Å			V_{cell}, Å^3		ρ_{theor}, g/cm^3		*R*-factors	
	Fe_2O_3		Ferrite	Fe_2O_3	Ferrite	Fe_2O_3	Ferrite	R_{wp}, %	R_{wpnb}, %
	a	*c*	*a*						
Ceramic Method 0.001	5.036± 0.001	13.740± 0.001	8.454±	301.740	604.125	5.273	5.298	2.18	19.19
Ceramic grinding 10 h	5.037± 0.001	13.746± 0.001	8.455± 0.001	301.97	604.423	5.269	5.295	2.13	19.25
Ceramic method + Co_3O_4 + CaO	5.036± 0.001	13.742± 0.001	8.464± 0.001	301.806	606.348	5.272	5.279	1.98	19.17
Ceramic method + Co_3O_4 + CaO, grinding 10 h	5.038± 0.001	13.745± 0.001	8.464± 0.001	301.965	606.377	5.269	5.278	2.02	21.14
Sol-gel	5.037± 0.001	13.744± 0.001	8.458± 0.001	301.975	605.020	5.269	5.202	2.19	19.78
Sol-gel, grinding 10 h	5.036± 0.001	13.740± 0.001	8.456± 0.001	301.728	604.522	5.273	5.206	2.31	20.94
Sol-gel + Co_3O_4 + CaO	5.037± 0.001	13.745± 0.001	8.465± 0.001	302.029	606.608	5.268	5.276	2.39	21.63
Sol-gel + Co_3O_4 + CaO, grinding 10 h	5.036± 0.001	13.742± 0.001	8.462± 0.001	301.793	605.868	5.272	5.283	2.12	21.03

hand, a decrease of the average grain size indicates the manifestation of the effect of reduction of the migration rate of grain boundaries because of the introduction of alloying additives, as shown in [17]. On the other hand, an increase in the number and size of abnormally large grains may indicate that there are local areas in ferrite in which the concentration of impurity elements and other defects is lower. The grain boundaries are less firmly fixed in such areas, which results in their accelerated movement during sintering. The parameter of the ferrite crystal lattice increases with the introduction of additives in the case of the ceramic and sol-gel method, which results in an increase of

Table 3. Properties of sintered ferrites

Method	ρ, g/cm^3	Average size grains excluding abnormally large grains, μm	Initial magnetic permeability μ_i			Maximum Induction B_m, mT (at $H_m = 1200$ A/m, $f = 10$ kHz)
			$T = 25°C$	$T = 100°C$	$T = 150°C$	
Ceramic method	4.65 ± 0.01	2.7 ± 0.1	1300 ± 100	2000 ± 200	2200 ± 100	420 ± 20
Ceramic method + Co_3O_4 + CaO	4.67 ± 0.02	2.4 ± 0.1	1600 ± 100	1900 ± 100	2200 ± 100	430 ± 20
Sol-gel method	4.89 ± 0.02	9.8 ± 0.4	1700 ± 100	2600 ± 200	3100 ± 200	490 ± 20
Sol-gel method + Co_3O_4 + CaO	4.79 ± 0.01	5.3 ± 0.1	1400 ± 100	1600 ± 100	1900 ± 100	450 ± 20

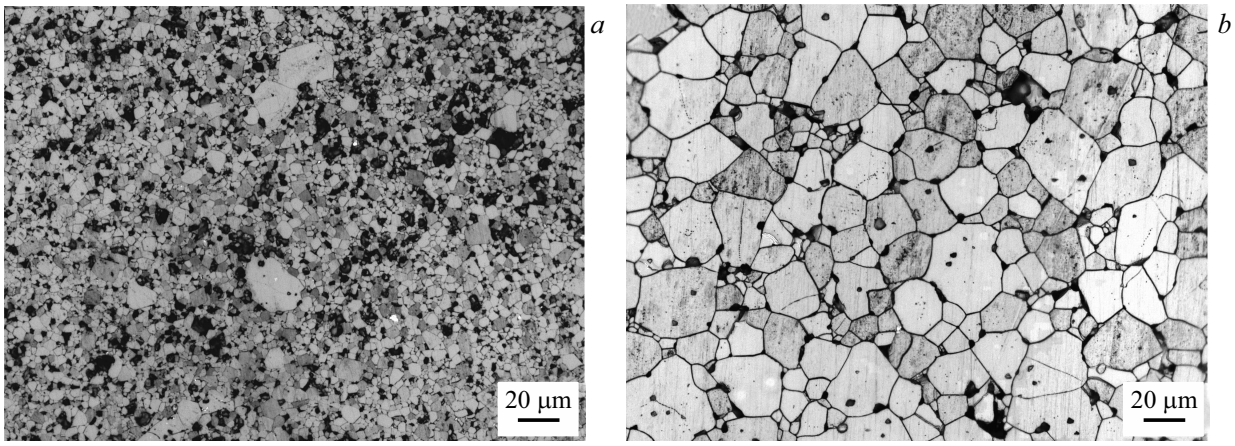

Figure 2. The microstructure of sintered ferrites. *a* — ceramic method with an addition of Co_3O_4+CaO; *b* — sol-gel method without additives.

the volume of the lattice cell implying a decrease of the theoretical density. This is attributable to the substitution of ions Fe^{3+} (0.67 Å) with ions Co^{2+} (0.82 Å) with a higher ion radius [18].

A 3.6-fold increase of the average grain size of ferrite obtained by the sol-gel method, compared with that for ferrite obtained using ceramic technology, indicates a higher activity of the powder during sintering (Fig. 2, *b*). Therefore, the growth of the average grain size during powder grinding is shown in [3]. The structure without abnormally large grains may be a consequence of the uniform distribution of components in the process of chemical synthesis. An increase of the average grain size and ρ contributed to an increase of μ_i by 30%. In addition, ferrite obtained using sol-gel synthesis shows the greatest growth of μ_i when heated from 25 to 150°C.

The additives containing 0.035 mass% Co_3O_4 and 0.05 mass% CaO in the case of sol-gel synthesis also contributed to a decrease of the average grain size by 10% and μ_i by 16% (Fig. 3, *a*). The containment of sintering processes by additives also resulted in a decrease of ρ and B_m. However, unlike the ceramic method, abnormal large grains have not formed, which confirms the uniformity of the distribution of additives.

The magnetic losses shown in Fig. 3, *b* at a low frequency of 10 kHz for Mn−Zn ferrites are primarily associated with hysteresis losses [19]. It is known that hysteresis losses depend on the ease of movement of domain boundaries in ferrite. The lowest level of losses is shown by the material obtained using the sol-gel synthesis method without additives. Because of the largest grain size, it has the smallest specific area of the boundaries, which prevent the movement of the domain walls. On the one hand, the increase of magnetic losses in case of the introduction of alloying components is associated with the grinding of the grain structure. On the other hand, Ca ions are known [17]not to dissolve in ferrite, instead they form a separate phase on the surface of ferrite grains, which also hinders the movement of domain boundaries.

Therefore, the work demonstrates the following.

— Sol-gel synthesis of Mn−Zn-ferrite powders results in an increase of the concentration of ferrite, the lattice parameter, and a decrease of the theoretical density and crystallite size of powders compared with the ceramic method.

— The concentration of ferrite and the size of the crystallite size powders decreased after grinding in a ball mill. Grinding resulted in an increase of the lattice parameters and a decrease of the theoretical density of powders

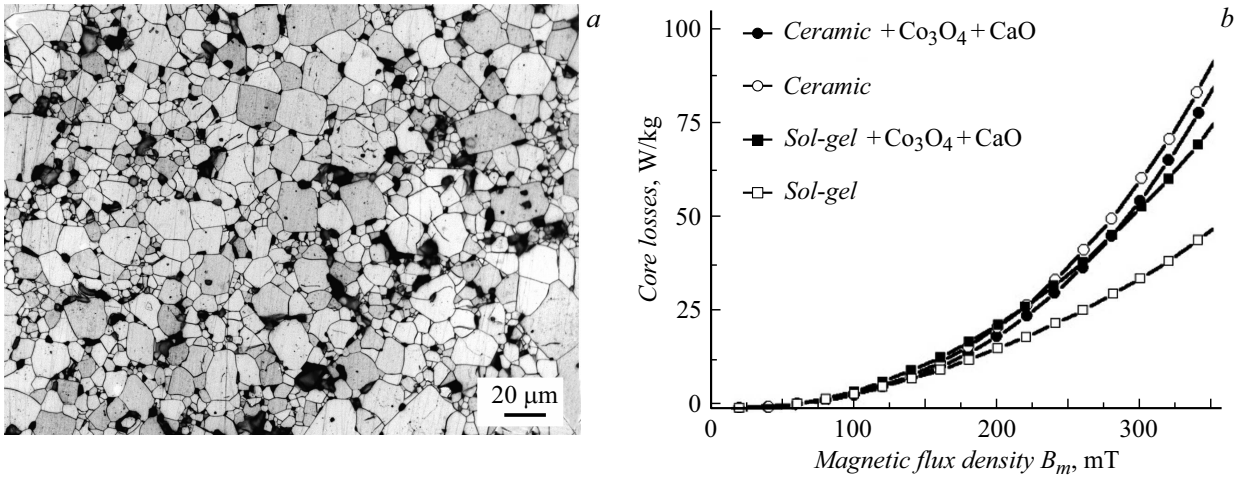

Figure 3. *a* — the microstructure of sol-gel ferrite with the addition of Co_3O_4+CaO; *b* — the dependence of magnetic losses on maximum induction B_m at the frequency of 10 kHz.

obtained using the ceramic method. The parameters decreased in the case of sol-gel synthesis, the theoretical density increased.

— The use of sol-gel synthesis made it possible to increase the density, initial magnetic permeability, average grain size, B_m at $H_m = 1200$ A/m, reduce magnetic losses at a frequency of 10 kHz compared with similar characteristics Mn–Zn ferrites obtained using ceramic technology.

— The addition of 0.035 mass% Co_3O_4 and 0.05 mass% CaO resulted in a decrease of the grain size, density, B_m at $H_m = 1200$ and/m, the initial magnetic permeability, an increase of magnetic losses at a frequency of 10 kHz.

The research was financially supported under the NSTU development program (scientific project № C23-30).

Funding

The studies were carried out on the equipment of core facility „Structure, mechanical and physical properties of materials“.

Conflict of interest

The authors declare that they have no conflict of interest.

References

[1] K. Li, C. Peng, K. Jiang, J. Hazard. Mater., **194**, 79 (2011). DOI: 10.1016/j.jhazmat.2011.07.060
[2] I. Szczygieł, K. Winiarska, A. Bieńko, K. Suracka, D. Gaworska-Koniarek, J. Alloys Compd., **604**, 1 (2014). DOI: 10.1016/j.jallcom.2014.03.109
[3] L. Wang, G. Lei, R. Cheng, C. Yan, H. Ge, Physica B, **552**, 6 (2019). DOI: 10.1016/j.physb.2018.09.035
[4] E.K. Papynov, O.O. Shichalin, V.Yu. Mayorov, E.B. Modin, A.S. Portnyagin, E.A. Gridasova, I.G. Agafonova, A.E. Zakirova, I.G. Tananaev, V.A. Avramenko, Ceram. Int., **43**, 8509 (2017). DOI: 10.1016/j.ceramint.2017.03.207
[5] E.K. Papynov, O.O. Shichalin, V.I. Apanasevich, A.S. Portnyagin, V.Yu. Mayorov, I.Yu. Buravlev, E.B. Merkulov, T.A. Kaidalova, E.B. Modin, I.S. Afonin, I.O. Evdokimov, B.I. Geltser, S.V. Zinoviev, A.K. Stepanyugina, E.A. Kotciurbii, A.A. Bardin, O.V. Korshunova, Powder Technol., **367**, 762 (2020). DOI: 10.1016/j.powtec.2020.04.040
[6] S.O. Aisida, M.H. Alnasir, S. Botha, A.K.H. Bashir, R. Bucher, I. Ahmad, T.-K. Zhao, M. Maaza, F.I. Ezema, Eur. Polym. J., **132**, 109739 (2020). DOI: 10.1016/j.eurpolymj.2020.109739
[7] F. Alam, M.L. Rahman, B.C. Das, A.K.M.A. Hossain, Physica B, **594**, 412329 (2020). DOI: 10.1016/j.physb.2020.412329
[8] Y.T. Chien, Y.C. Ko, J. Mater. Sci., **26**, 5859 (1991). DOI: 10.1007/BF01130125
[9] L. Sun, J. Guo, Q. Ni, E. Cao, Y. Zhang, W. Hao, L. Ju, J. Mater. Sci.: Mater. Electron., **29**, 5356 (2018). DOI: 10.1007/s10854-017-8501-2
[10] T. Tangcharoen, A. Ruangphanit, W. Pecharapa, Ceram. Int., **39**, 239 (2013). DOI: 10.1016/j.ceramint.2012.10.069
[11] L. Lutterotti, Nucl. Instrum. Meth. Phys. Res. B, **268**, 334 (2010). DOI: 10.1016/j.nimb.2009.09.053
[12] V.G. Kostishin, I.I. Kaneva, V.G. Andreev, A.N. Nikolaev, E.I. Volkova, Izv. vuzov. Materialy elektronnoy tekhniki , **1, 23** (2013), 137 (2022). (in Russian).
[13] M.J.N. Isfahani, M. Myndyk, V. Šepelák, J. Amighian, A. Mössbauer, J. Alloys Compd., **470**, 434 (2009). DOI: 10.1016/j.jallcom.2008.02.113
[14] A. Hajalilou, M. Hashim, M. Taghi Masoudi, Ceram. Int., **41**, 8070 (2015). DOI: 10.1016/j.ceramint.2015.03.005
[15] L. Nalbandian, A. Delimitis, V.T. Zaspalis, E.A. Deliyanni, D.N. Bakoyannakis, E.N. Peleka, Micropor. Mesopor. Mater., **114**, 465 (2008). DOI: 10.1016/j.micromeso.2008.01.034
[16] S. Bid, S.K. Pradhan, Mater. Chem. Phys., **84**, 291 (2004). DOI: 10.1016/j.matchemphys.2003.08.012
[17] T. Akashi, Trans. Jpn. Inst. Met., **2**, 171 (1961). DOI: 10.2320/matertrans1960.2.171
[18] Q. Zhang, P. Zheng, L. Zheng, J. Zhou, H. Qin, J. Electroceram., **32**, 230 (2014). DOI: 10.1007/s10832-013-9878-9
[19] G. Kogias, V. Tsakaloudi, P. Van Der Valk, V. Zaspalis, J. Magn. Magn. Mater., **324**, 235 (2012). DOI: 10.1016/j.jmmm.2011.07.055

Translated by A.Akhtyamov